RSC Advances

ROYAL SOCIETY OF CHEMISTRY

www.rsc.org/advances

Table of Content

An efficient Vanillinyl Schiff base as a turn on fluorescent probe for Zinc(II) and Cell imaging

Anup Kumar Bhanja, Chiranjit Patra, Sudipa Mondal, Durbadal Ojha, Debprasad Chattopadhyay, Chittaranjan Sinha*

Vanillinyl Schiff base (H_2L), a nontoxic probe and a fluorescent sensor to Zn^{2+}, LOD 0.018 μM is used for living cell imaging.

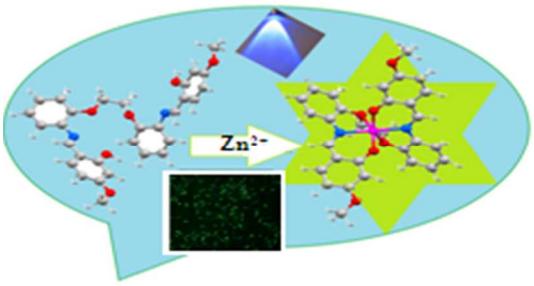

An efficient Vanillinyl Schiff base as a turn on fluorescent probe for Zinc(II) and Cell imaging

Anup Kumar Bhanja[a], Chiranjit Patra[a], Sudipa Mondal[a], Durbadal Ojha[b], Debprasad Chattopadhyay[b], Chittaranjan Sinha[a]*

6,6′-((1Z,1′Z)-(((Ethane-1,2-diylbis(oxy))bis(2,1-phenylene))bis(azanylylidene))bis(methanylylidene))bis(3-methoxyphenol), a vanillinyl Schiff base, shows unprecedented fluorescent zinc sensing property and has been examined for zinc bioimaging. Zinc induced turn-on fluorescence enhancement is observed at 472 nm and steady state photophysical studies establish the metal promoted deprotonation and chelation enhancement of emission. Formation of the 1:1 metal-to-ligand complex has been ascertained by ^{1}H NMR, mass spectral analysis and Job's plot. Limit of detection (LOD) is the lowest, 0.018 μM in the family of fluorogenic Zn^{2+}-sensors. Apart from this, theoretical interpretation of the experimental outcome has also been obtained by applying density functional theory (DFT) to the ligand and the complex. The practical applicability of the ligand has been examined in living cells (African Monkey Vero Cells). MTT assay proves the no toxicity of probe upto 300 μg/ml.

[a]Department of Chemistry, Jadavpur University, Kolkata 700 032, India, c_r_sinha@yahoo.com

[b]ICMR Virus Unit, Infectious Diseases & Beliaghata General Hospital, GB-4, 57, S. C. Bannerjee Road, Beliaghata, Kolkata – 700 010, debprasad@gmail.com

Introduction

Zinc is the constituent of more than 250 metallo-biomolecules and is the second abundant transition metal ion in the human body.[1-4] Zinc deficiency causes acrodermatitis enteropathica,[5] prostate cancer, diabetes, and brain diseases while its excess may cause serious neurological disorders such as Alzheimer's and Parkinson's diseases.[6,7] Zinc dependency of environmental and biological systems created a need for the development of selective techniques for its detection. Different methods for the detection of zinc ions have been proposed, such as atomic absorption spectrometry,[8] inductively coupled plasma mass spectroscopy (ICPMS),[9] inductively coupled plasma–atomic emission spectrometry (ICPAES),[10] and voltammetry.[11] Fluorimetry is becoming a powerful tool for its simplicity and specificity[12,13] and a useful choice of estimation of biological ion concentration.[14] Because of $3d^{10}$ electronic configuration, Zn^{2+} is spectroscopically silent and numerous fluorescent sensors have been characterized to determine its concentration in living cells over the last decade. [15-24] In particular imine based sensors have drawn special attention.[25] Here in, we have synthesised a, 6,6′-((1Z,1′Z)-(((Ethane-1,2-diylbis(oxy))bis(2,1-phenylene))bis (azanylylidene))bis(methanylylidene))bis(3-methoxyphenol), (H_2L), by the condensation of 2-hydroxy-4-methoxy-benzaldehyde (HMB) and 2,2'-(ethane-1,2-diylbis(oxy))dianiline (EDOD). The ligand, H_2L acts as a fluorescent zinc sensor based on the metal promoted deprotonation followed by chelation enhancement of emission. The composition of the complex has been supported by spectroscopic data (IR, Mass, Job's plot, ^{1}H NMR). The DFT computation of optimised geometry of H_2L and the complex has been used to explain the electronic spectral properties. The practical applicability of the ligand (H_2L) has been tested in African green monkey kidney cells (Vero cells, ATCC, Manassas, VA, USA) for the determination of exogenous zinc ions by fluorescence cell imaging processes.

Experimental

Material and methods

All reagents and solvents used for synthesis were from commercial sources and used as received. All aqueous solutions were prepared using Milli-Q water (Millipore). 2-(Hydroxy)-4-(methoxy)-benzaldehyde (HMB) was purchased from Sigma-Aldrich and 2,2′-(ethane-1,2-diylbis(oxy))dianiline (EDOD) was prepared following reported procedure.[26] $ZnCl_2$ was obtained from E. Merck, Germany. All other solvents and chemicals were purchased from Merck (AR grade) and used without further purification. ^{1}H NMR (300 MHz) was recorded from a Bruker (AC) 300 MHz FT-NMR spectrometer using TMS as an internal standard. UV–Vis spectra were collected from a Perkin Elmer Lambda 25 spectrophotometer and the fluorescence spectra were obtained from Perkin Elmer Spectrofluorimeter model LS55 at room temperature; FT-IR spectra (KBr disk, 4000–400 cm^{-}1) from a Perkin Elmer LX-1 FTIR spectrophotometer.

Preparation of 6,6′-((1Z,1′Z)-(((Ethane-1,2-diylbis(oxy))bis(2,1-phenylene))bis (azanylylidene))bis(methanylylidene))bis(3-methoxyphenol), (H_2L)

The synthesis was carried out following modification of reported method.[26] To methanol solution (10 ml) of 2-(hydroxy)-4-(methoxy)-benzaldehyde (HMB) (0.17 g, 1 mmol) was added 2,2'-(ethane-1,2-diylbis(oxy))dianiline (EDOD) (0.244 gm, 1 mmol) in dropwise with stirring. The reaction mixture was then refluxed for 2 hours and then cooled down to room temperature. Yellow crystalline precipitate deposited and was filtered, washed by MeOH to isolate H_2L. It was then dried and recrystallized from hot methanol in the yield of 70%. M. pt., 190°c; Microanalytical data $C_{30}H_{28}N_2O_6$: Anal. Found: C, 70.22; H, 5.54; N, 5.42%; Calc.: C, 70.30; H, 5.51; N, 5.51%. ^{1}H-NMR (300 MHz, $CDCl_3$) : δ 14.31 (s, 2H, OH), 8.82 (s, 2H, imine-H, 2H), 6.34 (d, 2H, J = 2.37 Hz, H_c), 6.43-6.40 (m, 2H, H_d), 7.05-7.00 (m, 2H,

H_e),7.20 (4H, d, J=3.75 Hz, H_f,H_j), 7.39-7.32 (m, 4H, H_g,H_i), 4.41 (s, 4H, -OCH_2), 3.75-3.78 (d, J=9.6 Hz,-OCH_3). FT-IR data (KBr pellet, cm^{-1}): 1619.45 cm^{-1} **,** 1242.82 cm^{-1}, ESI-MS (M^++H), 513.198 .

DFT computation

Geometry optimization of H_2L and [ZnL] complex were performed by DFT/B3LYP method using Gaussian 09 software.[27-29] 6-311+(d, p) basis set were used for C, H, N, O and Lanl2dz basis set was used as effective potential (ECP) set for Zn.[30-32] The vibrational frequency calculations were performed to ensure that the optimized geometries represent the local minima and there are only positive eigen values. Theoretical UV-Vis spectra were calculated by time-dependent-DFT/B3LYP method in methanol using conductor-like polarizable continuum model (CPCM).[33-35] GAUSSSUM[36] was used to calculate the fractional contributions of various groups to each molecular orbital.

Immunofluorescence (IFA) studies

African green monkey kidney cells (Vero cells, ATCC, Manassas, VA, USA) was grown and maintained in Eagle's minimum essential medium (EMEM), supplemented with 5–10% fetal bovine serum (FBS). Vero cells monolayer (1.0×10^6 cells/ml) was grown onto 6 well plates at 5% CO_2 for 24h. The cells were then fixed with paraformaldehyde (4%) and blocked with 1% bovine serum albumin (BSA) in 0.1% PBS-triton X100 solution. The cells were washed with PBS, and then permeabilized with 0.1% Triton-X100 in PBS. Permeabilized Vero cells monolayer treated with H_2L (100 µg/ml) for 1h at room temperature was washed twice with phosphate buffered saline (PBS, pH 7.2) to remove the cell debris. After washing with PBS, Zn^{2+} (100 µg/ml) was added for 10 min, and washed twice with PBS. Then, the cells were observed under epifluorescence microscope.[37]

Cell Cytotoxicity assay

The cytotoxic effects of H_2L, $ZnCl_2$ were determined by an MTT (3-[4,5-dimethylthiazol-2-yl]-2,5 diphenyl tetrazolium bromide) assay following the manufacturer's instruction (MTT 2003, Sigma-Aldrich, MO). This assay is based on the conversion of MTT into formazan crystals by mitochondrial dehydrogenases of living cells to cleave the tetrazolium rings of MTT to form dark purple membrane impermeable crystals of formazan that can be measured at 540 nm after solubilization in DMSO. This assay is broadly used to measure the in vitro cytotoxic effects of drugs on cell lines. African green monkey kidney cells were cultured into 16-well plates (approximately 1.0×10^6 cells/ml) for 24 h. Next day various concentrations of probe (0, 50, 100, 200, 300, 400, 500 μM) made in EMEM (Eagle's minimum essential medium) were added to the cells and incubated for 24 h. Solvent control samples (cells treated with DMSO in EMEM). Following incubation and fresh EMEM containing MTT solution was added. The plate was incubated for 3–4 h at 37°C. Subsequently, the supernatant was removed, the insoluble colored formazan product was solubilized in DMSO, and its absorbance was measured. The OD value of wells containing only EMEM medium was subtracted from all readings to get rid of the background influence. Data analysis and calculation of standard deviation were performed with Microsoft Excel 2007 (Microsoft Corporation).

Results and Discussion

Vanillinyl Schiff base, 6,6′-((1Z,1′Z)-(((Ethane-1,2-diylbis(oxy))bis(2,1-phenylene))bis(azanylylidene))bis(methanylylidene))bis(3-methoxyphenol) (**Scheme 1**), has been characterised by spectroscopic (FT-IR, UV-Vis, ^{1}H NMR, Mass) data. IR spectrum shows ν(C=N) at 1619 cm^{-1} (**Supplementary Material, Fig. S1**)**;** Mass ion peak at 513.19

corresponds to $(M+H)^+$ (**Supplementary Material**, **Fig. S2**); the ^1H NMR spectrum shows singlet δ(OH) at 14.31 ppm, imine-H, δ(CH=N) at 8.82 ppm and other aromatic protons have been assigned based on their spin-spin interaction and on comparing with the spectra of precursors (**Supplementary Material, Fig. S3**). The UV-Vis spectrum of H_2L in DMSO/water (HEPES buffer, pH = 7.4; v/v, 3/7) shows intense absorption at 286 and 346 nm those are assigned to π-π* and n-π* transitions.

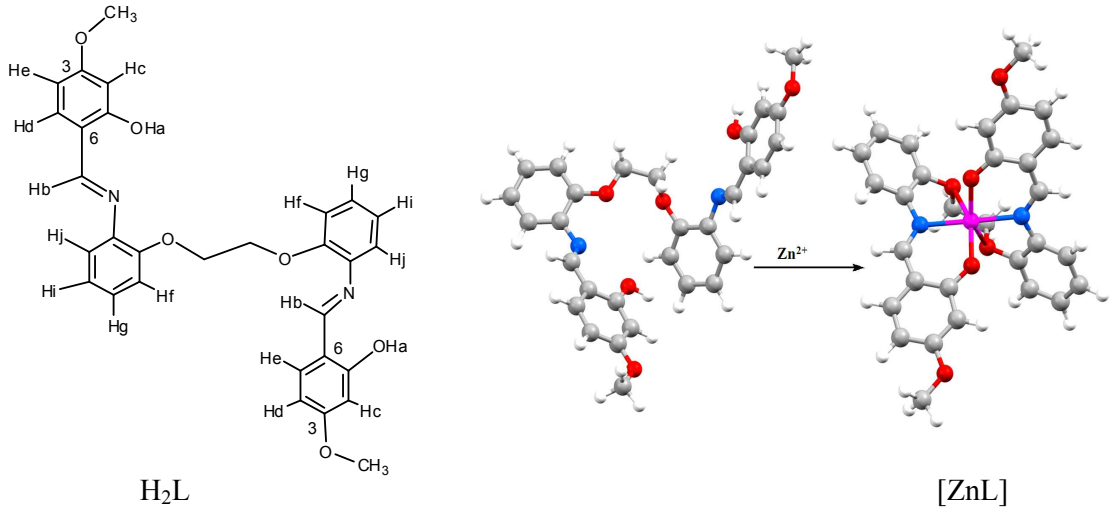

H_2L [ZnL]

Scheme 1. H_2L and proton labelling; optimized structures of H_2L and [ZnL]

Zn^{2+} Induced Absorption Spectroscopic study

The interaction of H_2L with Zn^{2+} has been examined by spectrophotometric titration at 25°C in DMSO/water (HEPES buffer, pH = 7.4; v/v, 3/7) mixed solution and shows a gradual development of new bands on increasing the addition of Zn^{2+} in the range 0-50 µm. The absorption at 286 and 346 nm of H_2L have been decreased gradually and an intense broad new band appears at 400 nm along with a band at 316 nm. Upon addition of other biologically abundant metal ions such as Na^+, K^+, Ca^{2+}, Mg^{2+}, Co^{2+}, Mn^{2+}, Ni^{2+}, Cu^{2+}, Fe^{2+} and Fe^{3+} and other metal ions like Pb^{2+}, Ba^{2+}, Hg^{2+}, Al^{3+} do not show any significant change of absorbance in the UV-VIS spectra of H_2L (**Supplementary Materials, Fig. S4**). No significant change

toward Cd^{2+} was observed even after addition of excess (~3 eqv.) of the above mentioned metal ions.

It is assumed that upon Zn^{2+} addition the bands of H_2L have been shifted to 316 and 400 nm respectively (**Fig. 1**). These observations suggest the undoubted conversion of free H_2L to the corresponding zinc complex. The appearance of isosbestic points also clearly indicates that the reaction is clean and straightforward (no side reaction, which may perturb isosbestic point). The red shifting of the bands of H_2L upon Zn^{2+} addition is attributed to an intramolecular charge transfer (ICT) through the chelation to Zn^{2+} forming ZnN_2O_4 distorted octahedral coordination with six-membered chelate ring *via* two nitrogen donor centres of C=N and two oxygen donors of vanillinyl phenolates along with five member chelate rings from two oxygen donor centres of ether group (**Scheme 1**). The increase of conjugation reduces the energy gap between the HOMO-LUMO and causes red shifting. The DFT computation of optimized structures of H_2L and [ZnL] has calculated the ΔE (LUMO-HOMO) 3.73 eV and 3.47 eV, respectively (*vide infra*) which supports the spectral observation. The absorbance shows a linear change until the molar ratio $[Zn^{2+}]$: $[H_2L]$ reaches 1 : 1, and no longer changes with further titration of Zn^{2+}. It is suggested that the stoichiometry between H_2L and Zn^{2+} is 1: 1, which is consistent with the results of the Job's plot (**Fig. 2**).

Fluorescence Spectroscopic Study

The fluorescence spectrum of H_2L with several cations (Na^+, Al^{3+}, Hg^{2+}, Cu^{2+}, Cd^{2+}, Co^{2+}, Mn^{2+}, Fe^{3+}, Pb^{2+}, Mg^{2+}, K^+, Ba^{2+}, Ni^{2+}, Zn^{2+}) using their chloride and acetate salts in DMSO/water (HEPES buffer, pH = 7.4; v/v, 3/7) solution have been examined on excitation at 346 nm (**Fig. 3**) and the turn-on emission is observed in presence of Zn^{2+} at room temperature (25°C). On increasing $[Zn^{2+}]$ to the solution of H_2L the fluorescence intensity

increases at 472 nm and becomes saturated on adding ~1.1 equivalent of Zn^{2+} which results 835 fold fluorescence enhancement in THF/methanol (v/v, 3/7) and 767 fold enhancement in DMSO/water (v/v, 3/7) (**Fig. 4**).

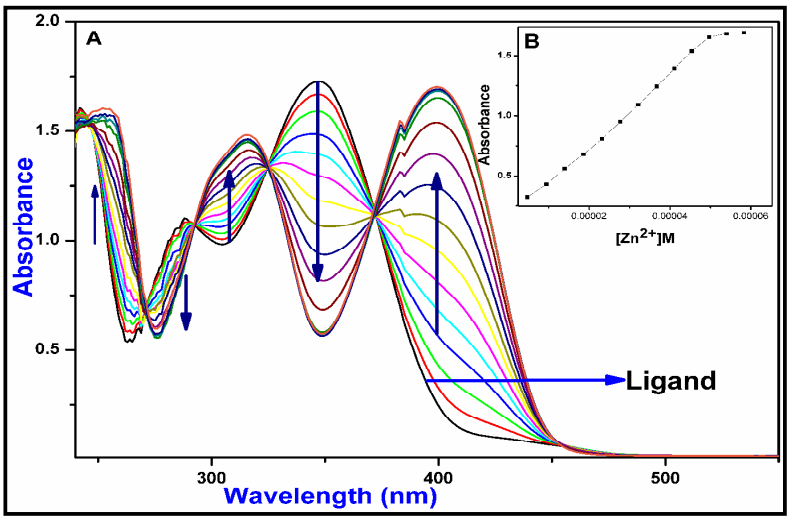

Fig.1. (A) Change in absorption spectra of H_2L (50 μM) upon addition of Zn^{2+} in DMSO/water (HEPES buffer, pH = 7.4, v/v, 3/7); (B) Non linear plot of absorbance (at 400 nm) vs. [Zn^{2+}] for the corresponding UV-Visible titration.

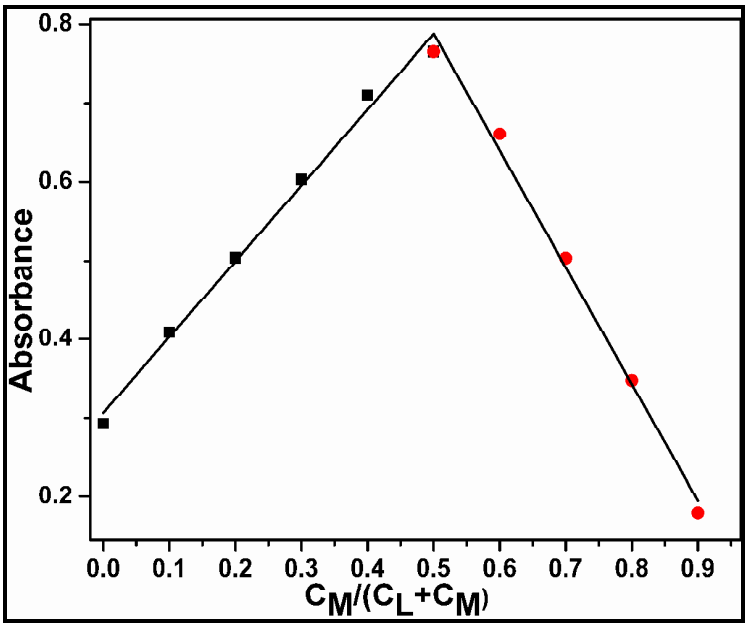

Fig. 2. The Job's plot shows 1 : 1 stoichiometry between [Zn^{2+}] and [H_2L]

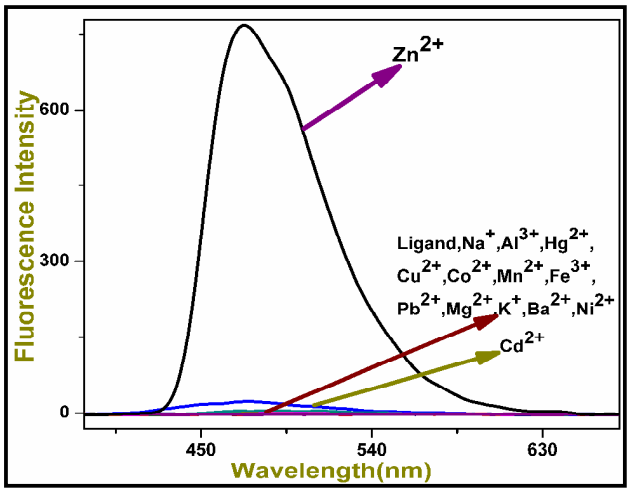

Fig. 3 : Fluorescence (λ_{ex} = 346 nm) responses of H_2L upon addition of various metal ions in DMSO/water (HEPES buffer, pH = 7.4; v/v, 3/7) at emission slit 7 nm

Selectivity is most important parameter for a fluorescent probe to a metal ion target. The detection of Zn^{2+} by the fluorescent probe has not been perturbed by biologically available metal ions like Na^{+}, K^{+}, Ca^{2+}; the Cd^{2+} shows a little perturbation while other interfering metal ions Co^{2+}, Mn^{2+}, Pb^{2+}, Ni^{2+}, Ba^{2+}, Mg^{2+}, Hg^{2+}, Al^{3+} become almost innocent towards fluorescence intensity change (**Fig. 4**). This is observed even after addition of 5 equivalents of the above mentioned interfering metal ions. The fluorescence intensity of probe (H_2L) is slightly quenched for Co^{2+}, Mn^{2+}, Ni^{2+}, Cu^{2+} and Fe^{3+} (**Fig. 4** and **Fig. 5**) which may be due to their paramagnetic character. Salen (*N*,*N*‘-bis(salicylidine)ethylenediaminato) type N_2O_2 chelating complexes of Fe^{2+} are model complexes for executing catalytic and biological studies.[38,39] Besides, iron is the most abundant transition metal in cellular systems. However, the probe, H_2L does not have any special selectivity to Fe^{2+} which has been examined by fluorescence spectroscopy and no significant change in band intensity is observed (**Supplementary Materials, Fig. S5**)

The dramatic fluorescence enhancement response to the binding of H_2L to Zn^{2+} (using $ZnCl_2$ solution) may be ascribed to (i) the deprotonation of phenolic-OH and the cause of restriction of excited-state induced proton transfer (ESIPT),[40-43] (ii) the prohibition of intramolecular electron-transfer process and (iii) the chelation-enhancement of fluorescence process along with lowering of vibrational loss due to rigid molecular structure of the complex.

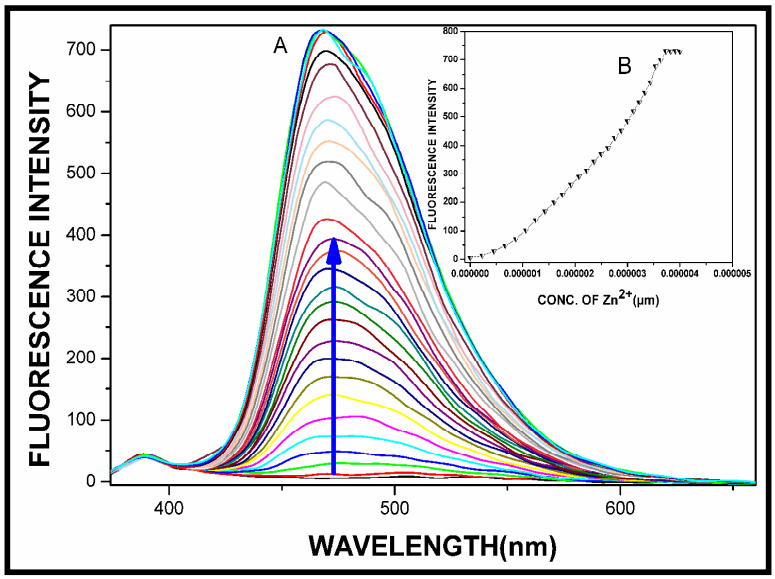

Fig. 4. (A) Change in fluorescence intensity of H_2L upon addition of 50 μM Zn^{2+} at emission slit 8 nm; (B) non-linear plot of fluorescence intensity (at 472 nm) *vs*. [Zn^{2+}] for the corresponding fluorescence titration.

H_2L exhibits a weak fluorescence with quantum yield (Φ_{H2L} =0.0026) in methanol, which was much lower than that (Φ_{ML} = 0.0113) in the presence of Zn^{2+} in THF/methanol (v/v, 3/7) medium. Similar experiment in DMSO/water (v/v, 3/7) mixture of H_2L shows comparable quantum yield (Φ_{H2L} = 0.0022) and in presence of Zn^{2+} ion in water enhances the quantum yield (Φ_{ML}) to 0.0125. The titration of Zn^{2+} in the solution of H_2L resulted in a remarkable increase in emission at 472 nm (**Fig. 4**) and visible change is very encouraging in UV-

chamber (**Supplementary Material, Fig. S6**). The binding constant (K_d) has been determined by fitting fluorescence data as a function of metal ion concentration to a suitable computer-fit nonlinear program (**Supplementary Material, Fig. S7**) and evaluated K_d, 12.45 x 10^4 $M^{-1}L$ in THF/methanol (v/v, 3/7) and 13.22 x 10^4 $M^{-1}L$ in DMSO/water (v/v, 3/7). The composition of the complex found to be 1:1 determined by Job's method (**Fig. 2**) and also further supported by mass spectrometric analysis (**Supplementary Material, Fig. S8**). The complex, [ZnL] is isolated from synthetic mixture and its infrared spectrum shows red shifting of ν(C=N) by 12 cm^{-1} compared to H_2L along with a new stretch at 490 cm^{-1} which is assigned to ν(Zn-O) (**Supplementary Material, Fig. S9**). The ^1H NMR spectrum of the complex also supports the chelation (**Supplementary Material, Fig. S10**).

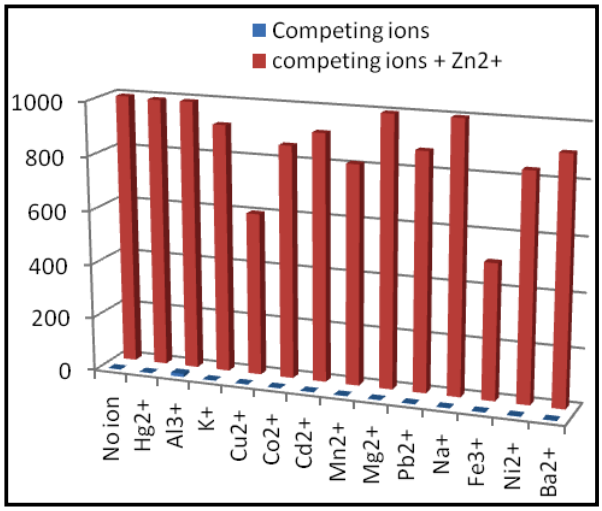

Fig. 5. Fluorescence intensity changes profiles of 100 μM H_2L in DMSO/water (HEPES buffer, pH = 7.4; v/v, 3/7) in presence of selected metal ions. The excitation wavelength was 346 nm and the emission slit at 10 nm.

The pH sensitivity of the emission of H_2L in absence and presence of Zn^{2+} has been examined by the acid–base titration (**Fig. 6**). H_2L or mixture of H_2L and Zn^{2+} in DMSO/water (v/v, 3/7) do not undergo any noticeable change in the fluorescence profile within the pH

range 2–6. In basic media (pH > 7), deprotonation of the phenolic group causes naked eye greenish yellow coloration along with green emission and highest emissivity is observed at pH, 11. Upon addition of Zn^{2+} the emission of H_2L shows highest intensity at pH, 10. This indirectly proves the suppression of ESIPT and causes enhancement of emission on coordination to Zn^{2+} followed by deprotonation of phenolato-OH.

The limit of detection (LOD) of Zn^{2+} has been determined by 3σ/m method and found to be as low as 0.018 μM (**Supplementary Material, Fig. S11**). Fluorescent sensors are well established and powerful tools for analytical quantification of molecules and ions in high precession and high accuracy level. Different chemical sensors based on different fluorogenic unit have been designed for Zn^{2+}-recognition such as pyrimidinyl based Schiff-base (LOD, 0.69 μM)[15], terphenyl-based motif (LOD, 0.10 μM)[44], 8-aminoquinolinyl derivatives (LOD, 1.85 μM[45]; 3.2 μM[16]), naphthyl fluorophore (LOD, 0.13 μM),[17] pyridyl system (LOD, 400 μM),[46] pyrenyl derivatives (LOD, 0.20 μM[47]; 0.08 μM[48]), porphyrinyl fluorophore (LOD, 0.055 μM).[49] All these facts indicate that H_2L behaves highly efficient fluorogenic chemosensor for Zn^{2+} recognition (LOD, 0.018 μM).

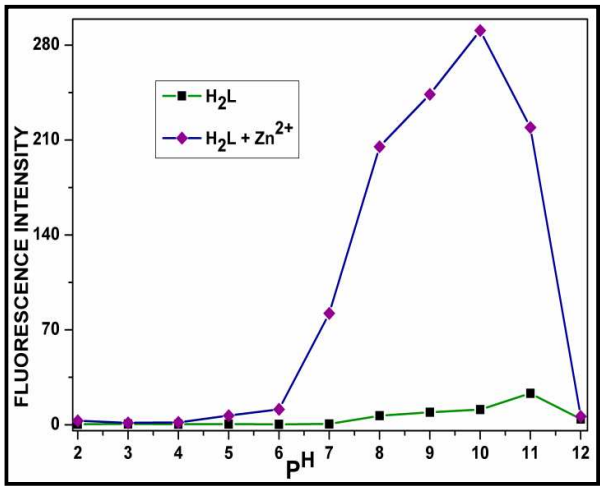

Fig. 6. Effect of pH on the fluorescence activity of H_2L and $H_2L$with Zn^{2+} in DMSO/water (v/v, 3/7)

Stoichiometric study by NMR Titration and Job's method

In order to support the binding of Zn^{2+} with the receptor H_2L, ^1H NMR titrations have been performed in DMSO-d_6. The titration curves showed a smooth and steady increase until a plateau was reached (**Fig. 7**). The ^1H NMR spectrum of H_2L contains signals (**Supplementary Material, Fig. S3**) for the OH, CH=N and aryl fragments at 14.31, 8.83 and 6.34–7.43 ppm, respectively. Addition of 0.5 equivalents of $ZnCl_2$ leads to a downfield shift of the signal corresponding to the CH=N proton ($\Delta\delta$ = 0.06 ppm) (**Fig. 7**). Furthermore, the signals of the aryl protons also exhibit dramatic changes; the aryl proton "e" arises at 7.73 ppm after addition one equivalent $ZnCl_2$. The co-ordination through phenolic oxygen atoms confirmed by NMR titration as the signal of phenolic oxygen proton (δ, 14.31 1.361 ppm) vanish after addition one equivalent $ZnCl_2$. Thus, according to the ^1H NMR titration data, interaction of H_2L with Zn^{2+} leads to the formation of a [ZnL] structure.

The Job's method of continuous variation of [Zn^{2+}] and [H_2L] in methanol has been performed by spectroscopic method measuring maximum absorbance at 400 nm and the plot of absorbance *versus* concentration ratio ($C_M/(C_L+C_M)$) indicates the 1 : 1 stoichiometry (**Fig. 2**). The mass spectrum of [ZnL] also shows molecular ion peak at 575.19 (**Supplementary Material, Fig. S8).**

Theoretical Studies

The DFT optimized structures of H_2L and [ZnL] have been generated following Gaussian09 software and the structural identity have been verified by calculating vibrational frequencies of some of the functions and on comparing with experimental spectra. The calculated metric parameters such as bond lengths of C=N (1.281 (H_2L); 1.325 (ZnL) Å), C-O (1.36 (H_2L) Å; 1.42 ([ZnL]) Å), Zn–N (2.131 Å), Zn–O(phenolic) (1.993 Å), Zn–O(ether) (2.492 Å) etc. and angles (∠N-Zn-O, 88.66°; ∠O-Zn-O, 88.67° etc. **Supplementary Materials, Table S1**) are

comparable with similar structures in literature[50] which exhibits Zn-N(imine), 2.151(2) Å; Zn-O(ether), 2.328(2) Å; Zn-O(phenolic), 2.020(2) Å and C=N, 1.317(3) Å. The binding of Zn^{2+} enhances the bond lengths of C=N and C–O which may be due to the electron drifting of metal ion from L^{2-}. This has been supported by red shifting of ligand dominated charge transfer transitions in the absorption spectra. The LUMO and other unoccupied MOs are composed from ligand function (>90%). The changes in the electronic properties of ligand on complexation with Zn^{2+} have been examined by the composition and energy of the MOs (**Supplementary Materials Table S2; Figs. S12, S13**). The energy difference between HOMO and LUMO is decreased from 3.73 eV in H_2L to the 3.47 eV in the complex, [ZnL] (**Fig. 8; Supplementary Materials, Table S3);** this supports the movement of absorption band to longer wavelength on coordination with Zn^{2+} (286 and 346 nm in H_2L shift to 316 and 400 nm respectively in [ZnL]). Ligand, H_2L has two equivalent parts of 2-hydroxy-4-methoxybenzylidene)amino)phenoxy)ethoxy)phenyl unit and the π-electrons of HOMO dominates one part of the symmetric H_2L while the complementary part electron density is running over LUMO (**Supplementary Materials, Fig. S10**). Thus HOMO→LUMO charge transition in H_2L refers to the intraligand charge transferences.

Phenols are strongly acidic at excited state, pK*< pK (pK, 10.6; pK*, 3.6).[13] Molecules of phenolic-OH may undergo excited state induced proton transfer (ESIPT) to the neighbouring hydrogen acceptor group and the radiative pathway is quenched. Addition of metal ion and its coordination followed by deprotonation may restrict ESIPT and may help emission. [ZnL] and the chelation enhancement of fluorescence (CHEF) contributes to the emission. Besides, the twisting of ligand geometry in chelated structure in a six-coordinated mononuclear complex will reduce the vibrational relaxation and improves the emission. The spectral transitions are assigned in **Fig. 9** and significant calculated bands are 362 nm ($S_0 \rightarrow S_2$) [HOMO-1→ LUMO (86%); f, 0.2995 (intraligand CT); experimental, 346 nm] and 290

nm ($S_0 \rightarrow S_6$) [HOMO-3→ LUMO (72%); f, 0.1216 (ILCT); experimental, 286 nm) for H_2L and 392 nm ($S_0 \rightarrow S_1$) [HOMO→LUMO(98%); f, 0.1013 (ILCT); experimental, 400 nm] and 331 nm ($S_0 \rightarrow S_4$) [HOMO-2→LUMO (82%); f, 0.4958 (ILCT)] for Zn^{2+}-L^{2-} complex.

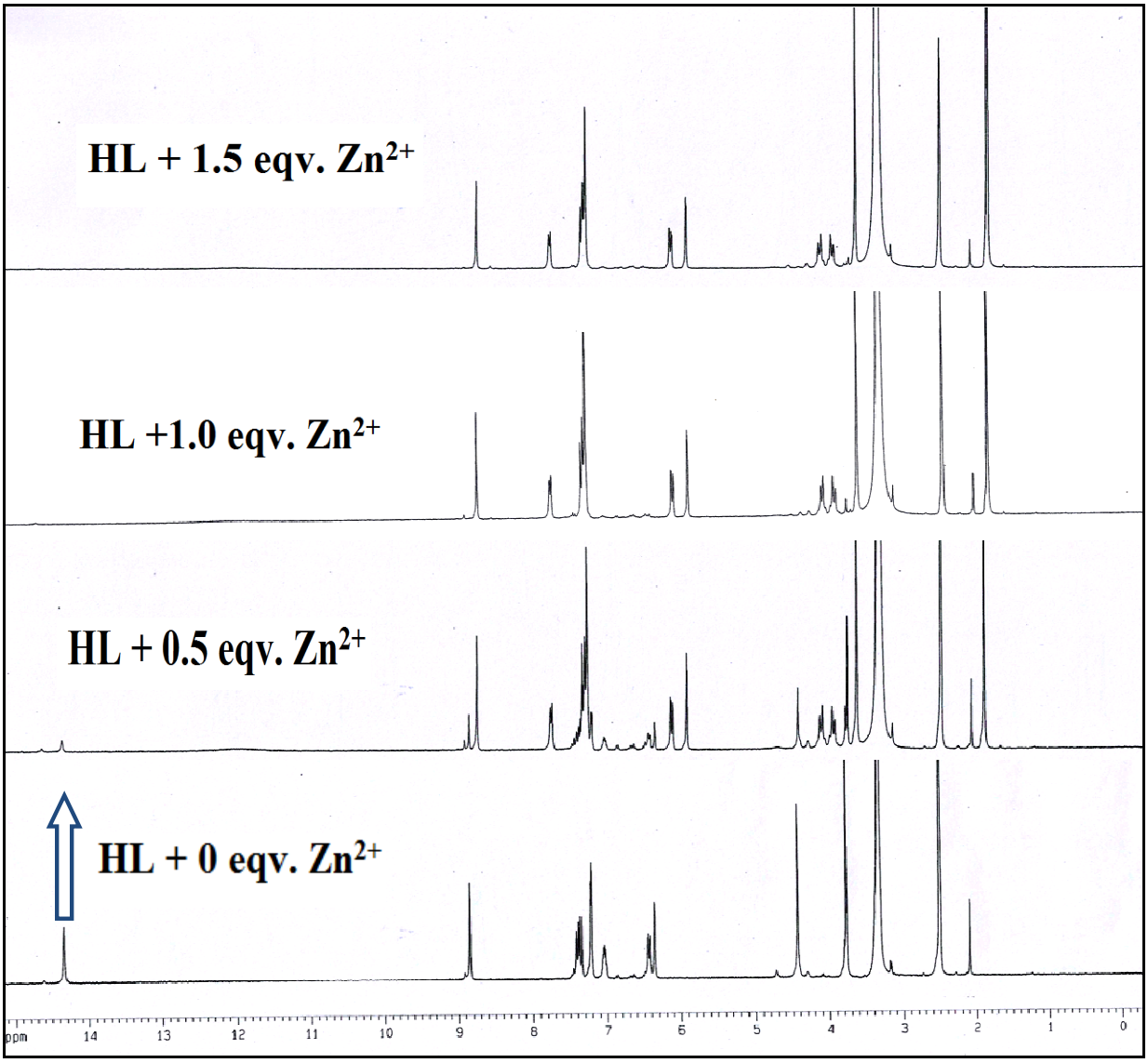

Fig. 7. ^1H NMR titration on adding $ZnCl_2$ solution to H_2L in DMSO-d_6

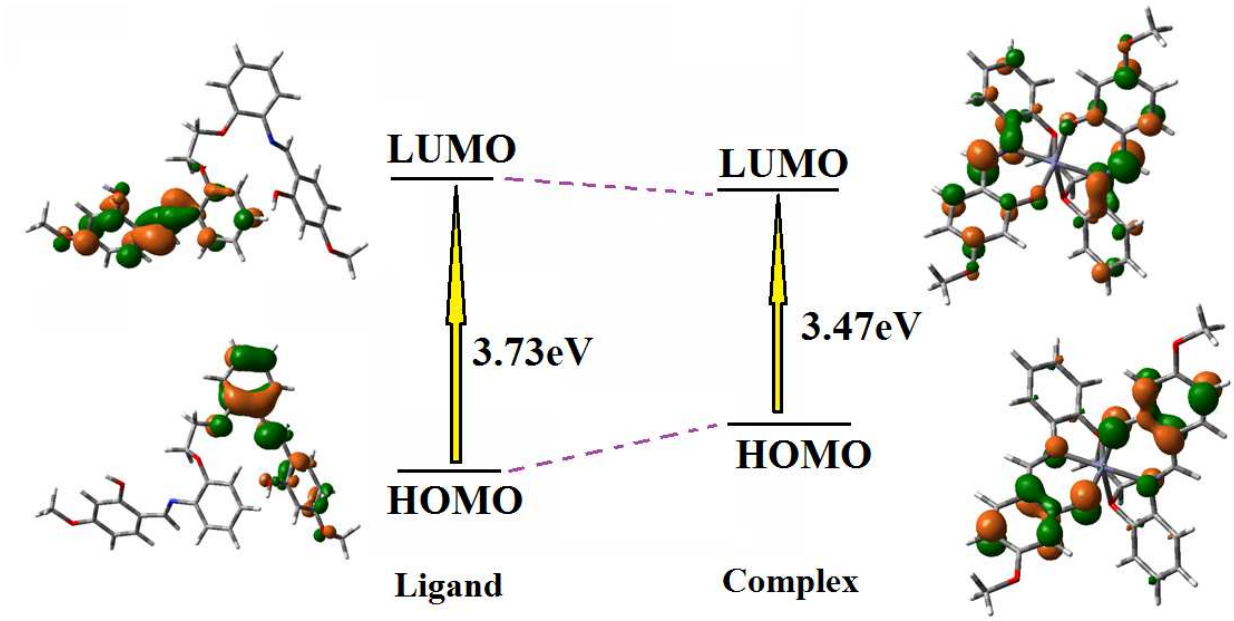

Fig. 8. Energy correlation of HOMO-LUMO gap between H_2L and [ZnL]

It is worth noting that Zn^{2+}-sensor with known fluorogenic unit in the binding side or in appended state such as pyridyl,[46] pyrimidinyl,[15] quinolineyl,[16, 45] pyrenyl,[47, 48] porphrinyl,[49] naphthyl,[17] etc. show low limit of detection. In this work vanillinyl Schiff base is not an effective fluorogenic substance but detects lowest LOD, 0.018 μM. The cavity size of the chelate ring, structural rigidity on twisting of the donor backbone and the suppression of ESIPT may contribute to high intense turn-on chemosensor behaviour.

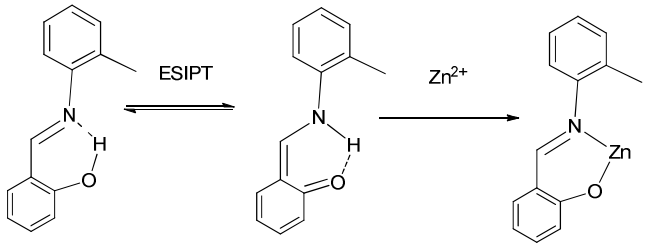

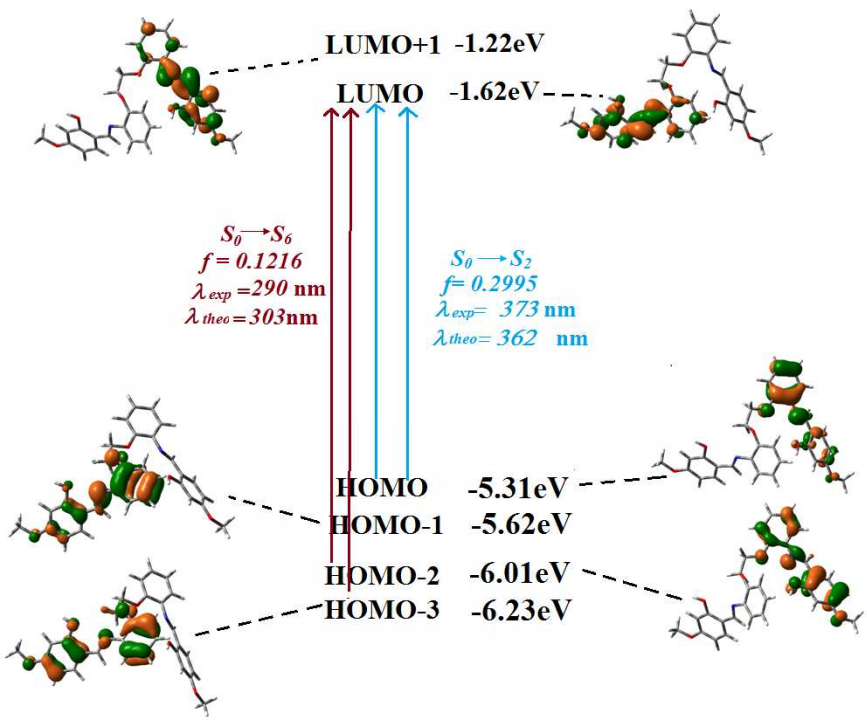

(a)

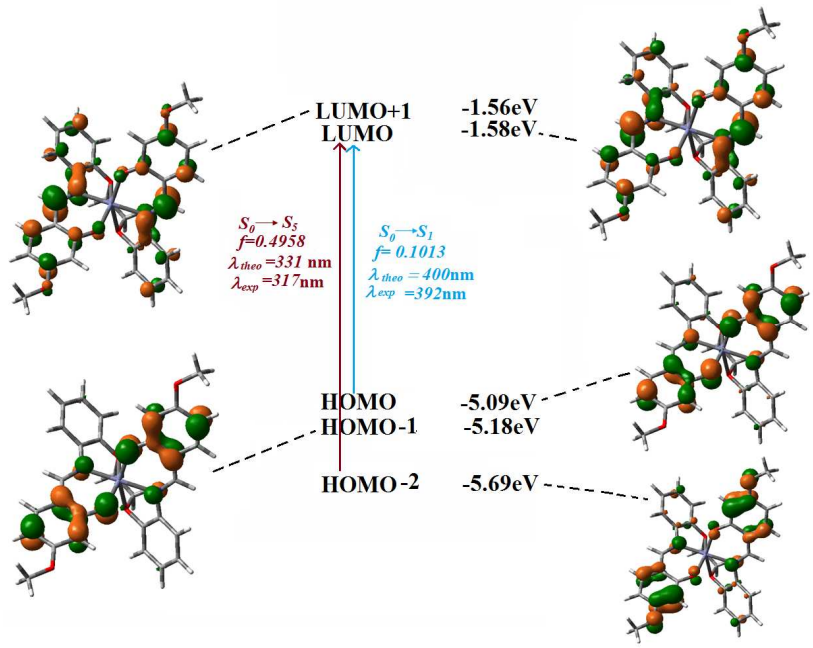

(b)

Fig 9. Assignment of calculated spectral transitions (a) H_2L and (b) [ZnL]

Cell Imaging Studies

The probe H_2L was applied to the detection of Vero cells (African green monkey kidney cells) to explore its utility in biological systems. The fluorescence imaging of intracellular Zn^{2+} in living cells is shown in **Fig.10**. Vero cells fixed in paraformaldehyde (4%) and blocked with BSA in PBS-triton X100 solution. Then, the cells were observed under epifluorescence microscope.[37] Then, the cells were treated with Zn^{2+} solution (30 mM) for 45 min in buffer for incubation, washed again with buffer at pH 7.4 and mounted on a grease free glass slide. Cells were observed under a fluorescence microscope equipped with a UV filter after adding H_2L (2 mM). Cells incubated only with Zn^{2+} were used as a control. H_2L can permeate easily through tested living cells without any harm (as the cells remain alive even after 30 min of exposure to H_2L at 2 mM). The MTT assay has been applied for labelling dead cells to evaluate cytotoxicity of the probe and is shown in **Fig. 11**. The study shows that H_2L has no cytotoxicity towards cells upto 300 μg/ml (approx). These results indicate that the probe has a huge potential in both *in vitro* and *in vivo* applications as a Zn^{2+} sensor and in live cell imaging

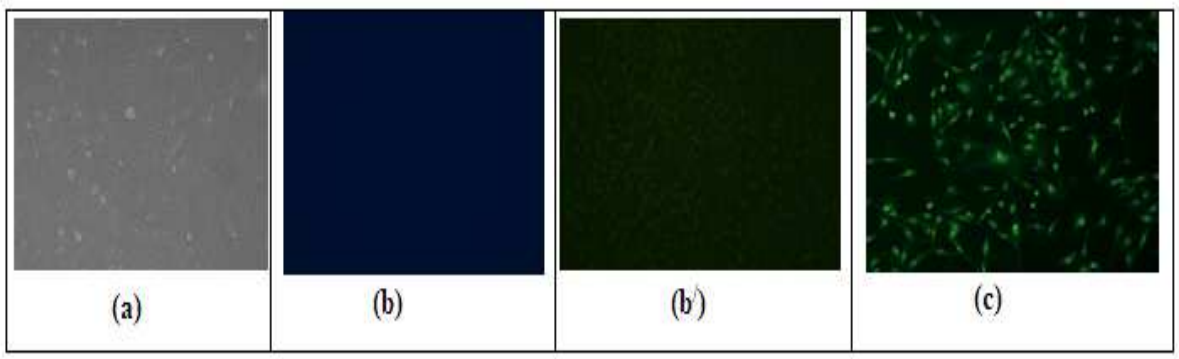

Fig. 10. Fluorescence microscope images of African Monkey Vero cells (a) Cell (control), (b) Cells incubated with H_2L, fluorescence image and (b/) bright field image, (c) Cells incubated with H_2L and Zn^{2+} solution

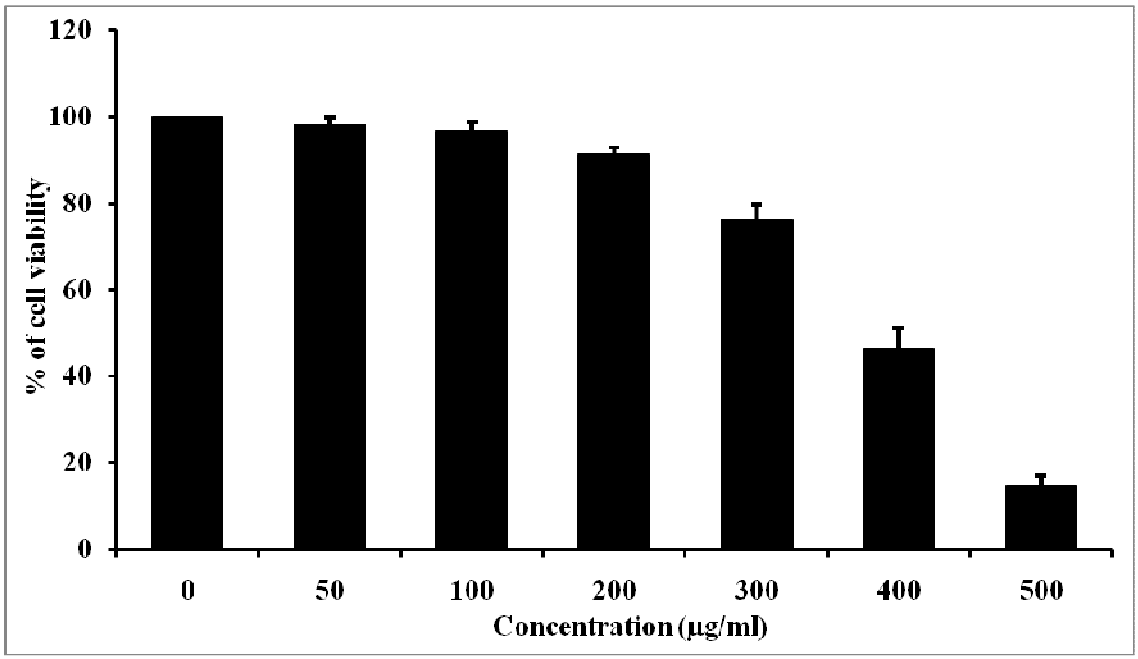

Fig. 11. Cell viability test by MTT assay by adding H_2L to the media

Conclusion

This work concerns with fluorogenic chemosensor for Zn^{2+}-recognition with vanillinyl Schiff base. The limit of detection is 0.018 μM and is the lowest in the series of aryl/heterocyclic fluorogenic Zn^{2+} sensor. Zinc induced turn-on fluorescence enhancement is observed at 472 which may specifically due to the cavity size of the chelate ring, structural rigidity on twisting of the donor backbone and the suppression of ESIPT. ^{1}H NMR, mass spectral analysis and Job's plot have supported the 1:1 metal-to-ligand complex formation. This technique has been used for imaging living cells (African Monkey Vero Cells) and the no toxicity of the probe has been checked by MTT assay.

Supplementary materials

The spectral data of H_2L (FT-IR, **Fig. S1**; Mass, **Fig. S2**; ^{1}H NMR, **Fig. S3**), Optical detection limit (**Fig. S4**), Benesi-Hildebrand plots (**Fig. S5**), Change in fluorescence intensity of H_2L

upon addition of 50 μM Fe^{2+} in DMSO/Water (**Fig. S6**), comparison of emission (**Fig. S7**), spectra of [ZnL] (Mass, **Fig. S8**; FT-IR, **Fig. S9**; ^{1}H NMR, **Fig. S10**), frontier molecular orbitals of H_2L (**Fig. S11**) and [ZnL] (**Fig. S12**), composition of MOs of [ZnL] (**Table S1**), comparison of theoretical and experimental spectral transitions and their assignment in H_2L and [ZnL] (**Table S2**), bond parameters of H_2L (**Table S3**) and [ZnL] (**Table S4**).

Acknowledgments

Financial support from the West Bengal Department of Science & Technology, Kolkata, India (Sanction No. 228/1(10)/(Sanc.)/ST/P/S&T/9G-16/2012) and the Council of Scientific and Industrial Research (CSIR, Sanction No. 01(2731)/13/EMR-II,), New Delhi, India are gratefully acknowledged. One of us (CP) thanks University Grants Commission, New Delhi, India for Fellowship.

References

1 J. M. Berg and Y. Shi, *Science*, **1996**, *271*, 1081–1085.

2 C. J. Frederickson and A. I. Bush, *Bio Metals*, **2001**, *14*, 353–366.

3. A. Voegelin, S. Pfister, A. C. Scheinost, M. A. Marcus and R. Kretzschmar, *Environ. Sci. Technol.*, **2005**, *39*, 6616–6623.

4. Y.. Tan, M. Liu, J. Gao, J. Yu, Y. Cui, Y. Yang and G. Qian, *Dalton Trans*., **2014**, *43*, 8048–8053

5. S. Kury, B. Dreno, S. Bezieau, S. Giraudet, M. Kharfi, R. Kamoun and J.-P. Moisan, *Nat. Genet.*, **2002**, *31*, 239–240.

6. M. P. Cuajungco and G. J. Lees, *Neurobiol. Dis*., **1997**, *4*, 137–169.

7. J.-Y. Koh, S. W. Suh, B. J. Gwag, Y. Y. He, C. Y. Hsu and D. W. Choi, *Science*, **1996**, *272*, 1013–1016

8. A. P. S. Gonzales, M. A. Firmino, C. S. Nomura, F. R. P. Rocha, P. V. Oliveira and I. Gaubeur, *Anal. Chim. Acta*, **2009**, *636*, 198 - 204.

9. J. S. Becker, A. Matusch, C. Depboylu, J. Dobrowolska and M. V. Zoriy, *Anal. Chem.,* **2007**, *79*, 6074 - 6080.

10. Y. Liu, P. Liang and L. Guo, *Talanta*, **2005**, *68*, 25 - 30.

11. A. A. Ensafi, T. Khayamian and A. Benvidi, *Anal. Chim. Acta*, **2006**, *561*, 225 – 232.

12. A. P. de Silva, H. Q. N. Gunaratne, T. Gunnlaugsson, A. J. M.Huxley, C. P. McCoy, J. T. Rademacher and T. E. Rice, *Chem. Rev.*,**1997**, *97*, 1515–1566.

13. B. Valeur, *Molecular Fluorescence: Principles and Applications*; Wiley-VCH: Weinheim, NY, **2002**.

14. E. Kimura and T. Koike, *Chem. Soc. Rev*., **1998**, *27*, 179 – 184.

15. S. S. Mati, S. Chall, S. Konar, S. Rakshit, S. C. Bhattacharya, *Sensors and Actuators*, *B*: *Chemical* **2014**, *201*, 204-212

16. S. Goswami, A. K. Das, K. Aich, A. Manna, S.Maity, K. Khanra and N.Bhattacharyya , *Analyst* , **2013**,*138*, 4593–4598

17. J. Guan, P. Zhang, T. Wei, Q. Lin, H. Yao and Y. –M. Zhang, *RSC Adv*., **2014**, *4*, 35797–35802

18. P. Li, X. Zhou, R. Huang, L. Yang, X. Tang, W. Dou, Q. Zhao and W. Liu, *Dalton Trans*., **2014**, *43*, 706–713

19. L. M. Hyman and K. J. Franz, *Coord. Chem. Rev*., **2012**, *256*, 2333–2356.

20. D. Buccella, J. A. Horowitz and S. J. Lippard, *J. Am. Chem. Soc*., **2011**, *133*, 4101–4114.

21 Z. Xu, K.-H. Baek, H. N. Kim, J. Cui, X. Qian, D. R. Spring, I. Shin and J. Yoon, *J. Am. Chem. Soc*., **2010**, *132*, 601–610.

22. G. Sivaraman, T. Anand and D. Chellappa, *Anal. Methods*, **2014**, *6*, 2343–2348.

23. M. Iniya, D. Jeyanthi, K. Krishnaveni, A. Mahesh and D. Chellappa, *Spectrochim. Acta, Part A,* **2014**, *120*, 40–46.

24. Y.Mikata, K. Kawata, S. Takeuchi, K. Nakanishi, H. Konno, S. Itami, K. Yasuda, S. Tamotsud and S. C. Burdette, *Dalton Trans*., **2014**, *43*, 10751–10759

25. Y. Liu, P. Liang and L. Guo, *Talanta*, **2005**, *68*, 25 - 30.

26. Y. Zhou, C. –Y. Zhu, X. –S. Gao, X. –Y. You, and C. Yao, *Org. Lett.,* **2010**, *12*, 2566-2569.

27. M.J. Frisch, G.W. Trucks, H.B. Schlegel, G.E. Scuseria, M.A. Robb, J.R. Cheeseman, G. Scalmani, V. Barone, B. Mennucci, G.A. Petersson, H. Nakatsuji, M. Caricato, X. Li, H.P. Hratchian, A.F. Izmaylov, J. Bloino, G. Zheng, J.L. Sonnenberg, M. Hada, M. Ehara, K. Toyota, R. Fukuda, J. Hasegawa, M. Ishida, T. Nakajima, Y. Honda, O. Kitao, H. Nakai, T. Vreven, J.A. Montgomery Jr., J.E. Peralta, F. Ogliaro, M. Bearpark, J.J. Heyd, E. Brothers, K.N. Kudin, V.N. Staroverov, R. Kobayashi, J. Normand, K. Raghavachari, A. Rendell, J.C. Burant, S.S. Iyengar, J. Tomasi, M. Cossi, N. Rega, J.M. Millam, M. Klene, J.E. Knox, J.B. Cross, V. Bakken, C. Adamo, J. Jaramillo, R. Gomperts, R.E. Stratmann, O. Yazyev, A.J. Austin, R. Cammi, C. Pomelli, J.W. Ochterski, R.L. Martin, K. Morokuma, V.G. Zakrzewski, G.A. Voth, P. Salvador, J.J. Dannenberg, S. Dapprich, A.D. Daniels, Ö. Farkas, J.B. Foresman, J.V. Ortiz, J. Cioslowski, D.J. Fox, GAUSSIAN 09, Revision D.01, Gaussian Inc., Wallingford, CT, **2009**.

28. A.D. Becke, *J. Chem. Phys*.,**1993**, *98*, 5648.

29. C. Lee, W. Yang, R.G. Parr, *Phys. Rev. B,* **1988**, *37*, 785 - 789.

30. P.J. Hay, W.R. Wadt, *J. Chem. Phys.*, **1985**, *82*, 270 - 283.

31. W.R. Wadt, P.J. Hay, *J. Chem. Phys.*, **1985**, *82*, 284-298.

32. P.J. Hay, W.R. Wadt, *J. Chem. Phys.*,**1985**, *82*, 299 - 305.

33. V. Barone, M. Cossi,. *J. Phys. Chem. A*, **1998**, *102*, 1995 – 2001.

34. M. Cossi, V. Barone, *J. Chem. Phys.*, **2001**, *115*, 4708 - 4717.

35. M. Cossi, N. Rega, G. Scalmani, V. Barone, *J. Comput. Chem*., **2003**, *24*, 669 - 681.

36. N.M. O'Boyle, A.L. Tenderholt, K.M. Langner, *J. Comput. Chem.*, **2008**, *29*, 839 - 845.

37. P. Bag, D. Chattopadhyay, H. Mukherjee, D. Ojha, N. Mandal, M. Sarkar Chawla, T. Chatterjee, G. Das and S. Chakraborti, *Virology J.*, **2012**, *9***,** 98-109.

38. G. Hilt, C. Walter and P. Bolze, *Adv. Synth. Catal.* , **2006**, *348*, 1241–1247

39. V. K. Sivasubramanian, M. Ganesan, S. Rajagopal, and R. Ramaraj, *J. Org. Chem.*, **2002**, *67*, 1506–1514

40. J. E. Kwon, S. Lee, Y. You, K. –H. Baek, K. Ohkubo, J. Cho, S. Fukuzumi, I. Shin, S. Y. Park, and W. Nam, *Inorg. Chem.*, **2012**, *51*, 8760–8774.

41. G. –J. Zhao, J.-Y. Liu, L.-C. Zhou, and K. –L. Han*, J. Phys. Chem. B ,* **2007**, *111,* 8940-8945 .

42. G. –J. Zhao and K. –L. Han, Acc. Chem. Res. **2012**, *45*, 404–413.

43. D. Yang, Y. Yang and Y. Liu, J. Clust. Sci., **2014,** *25*, 467–481.

44. V. Bhalla, R. Tejpal and M. Kumar, *Dalton Trans*., **2012**, *41*, 10182–10188.

45. Y. Li, J. Wu, X. Jin, J. Wang, S. Han, W. Wu, J. Xu, W. Liu, X. Yao and Y. Tang, *Dalton Trans.,* **2014**, *43*, 1881–1887.

46. T. Mukherjee, J. C. Pessoa, A. Kumar and A. R. Sarkar, *Dalton Trans.*, **2012**, *41*, 5260–5271.

47. S. A. Ingale, F. Seela , *J. Org. Chem.*, **2012**, *77*, 9352-9356.

48. P. Thirupathi , K. H. Lee, , *Bioorg. Med. Chem. Lett.*, **2013**, *23*, 6811-6815.

49. C. Y. Li, X. B. Zhang, Y. Y. Dong, Q. J. Ma, Z. X. Han, Y. Zhao , G. L. Shen, R. Q. Yu, *Anal Chim Acta*, **2008**, *616*, 214-221.

50. G. Rajsekhar, C. P. Rao, P. Saarenketo, K. Na¨ttinenb and K. Rissanen, New. J. Chem., **2004**, *28*, 75-84.